# Electrocatalytic reduction of nitrite on a polycrystalline rhodium electrode

M. Duca [a,*], B. van der Klugt [a], M.A. Hasnat [b,c], M. Machida [c], M.T.M. Koper [a]

[a] Leiden Institute of Chemistry, Leiden University, P.O. Box 9502, 2300 RA Leiden, The Netherlands
[b] Department of Chemistry, Graduate School of Physical Sciences, Shahajalal University of Science and Technology, Sylhet 3114, Bangladesh
[c] Department of Nano Science and Technology, Graduate School of Science and Technology, Kumamoto University, 2-39-1 Kurokami, Kumamoto 860-8555, Japan

## ARTICLE INFO

## ABSTRACT

This paper addresses the mechanism of the electrochemical reduction of $HNO_2$ and $NO_2^-$ on polycrystalline rhodium. Intermediates and/or reaction products were detected by means of various (combined) techniques: rotating ring-disk voltammetry (for $NH_2OH$ detection), online electrochemical mass spectrometry (for volatile products) and transfer experiments (for $NO_{ads}$). In acidic media, $HNO_2$ depletion due to homogeneous-phase reactions generates dissolved NO: the latter species can be adsorbed at Rh and is reduced to $N_2O$ when $0.3 < E < 0.5$ V (vs. RHE), while $HNO_2$ is reduced in a diffusion-limited wave to mainly $NH_3$ at potentials preceding hydrogen evolution. In alkaline media, the predominant product for the reduction of $NO_2^-$ when $E < 0.2$ V is still $NH_3$, which can poison the electrode via dehydrogenation to $NH_{x,ads}$ species. For more positive potentials, reduction still occurs via $NO_{ads}$ and stops at $NH_2OH$ for $E > 0.3$ V. The behavior of Rh is compared to Pt and explained in terms of general properties of these metals. A mechanistic scheme including NO, $HNO_2$ and $NO_2^-$ is discussed.

## 1. Introduction

Among the inorganic molecules involved in the nitrogen cycle, nitrite and nitrate are regarded with particular interest, and their levels in groundwater are kept under close scrutiny [1] given their potential toxicity [2]. These anions are targeted by various waste-water remediation techniques [3–7], with (electro)catalytic processes [8] still needing further improvement to avoid undesired byproducts such as $N_2O$ or $NH_3$.

In fundamental research, nitrite is also an interesting species, being central to the so-called electrochemical nitrogen cycle [9] as intermediate of $NO_3^-$ reduction [10] or NO oxidation [11]. In aqueous solutions, this anion displays pH-dependent homogeneous-phase equilibria, such as the acid–base equilibrium $HNO_2/NO_2^-$ ($pK_a = 3.16$ [12], 3.37 [13]). Therefore, the main species changes with the pH, $NO_2^-$ predominating in neutral/alkaline pH media, while $HNO_2$ is the dominant species at pH < 2. This fact is highly relevant from an electrochemical point of view, as shown by the completely different response of a polycrystalline platinum electrode in the two pH regions [14]. Besides, $HNO_2$ is involved in acid-catalyzed decomposition reactions [9,14,15] which generate, among others, NO. NO is known to be reactive at metal electrodes [9], and its influence on Pt electrochemistry in $HNO_2$ solutions of low pH was reported recently [14].

Being the most expensive noble metal, as catalyst for practical purposes rhodium should be used as a dispersed phase on a substrate [16–18], as a coating on a supporting material [19] or in mixed metal cathodes with Pd and Pt [20]. For example, in a study dealing with the electrochemical abatement of nitrates in alkaline media [19], Rh was electrodeposited on Ti foils and subsequently electrochemically activated. The morphological changes thus achieved ensured an enhancement of nitrate reduction over hydrogen evolution with a remarkably high selectivity to $N_2$, albeit under conditions of extensive continuous potential cycling. From a more fundamental point of view, the electrochemistry of nitrogen-containing molecules on (single-crystal and polycrystalline) rhodium electrodes has been investigated in various studies [9]. Significant to this work is that rhodium is the most active noble- or coinage-metal for the electroreduction of $NO_3^-$ ions in acidic media [10] and that in neutral media nitrite reduction on rhodium is faster than nitrate reduction [16]. Tafel slope values close to 120 mV dec$^{-1}$ indicated that, similarly to Pt, the first electron transfer (to give $NO_2^-$) is the rate-determining step (r.d.s.) [10]. However, no evidence for the formation of gaseous products (NO, $N_2O$, $N_2$) was found [10], pointing to the formation of soluble products only ($NH_3OH^+$ and $NH_4^+$).

Only a few works directly dealing with $HNO_2/NO_2^-$ reduction on Rh have thus far been published, covering the acidic [20–22] and the neutral/alkaline pH range [16,20]. The relevance of $HNO_2/NO_2^-$ reduction for the nitrogen-cycle electrocatalysis on Rh lies in the fact that, for the reduction of nitrate, the reaction steps following the first electron transfer ($NO_3^- \rightarrow NO_2^-$) will more likely determine the

* Corresponding author.
  E-mail address: m.duca@chem.leidenuniv.nl (M. Duca).

selectivity of the overall nitrate reduction. With regard to the determination of the intermediates of nitrous acid reduction, the comparison of single-crystal (basal planes) Pt and Rh electrodes was carried out by Rodes et al. [21] with combined electrochemical and spectroscopic techniques (Fourier-Transform Infrared Spectroscopy, FTIRS). Cyclic voltammetry proved that the onset of the reduction process, ascribed to the reduction of both adsorbed species and solution $HNO_2$, occurred at a less positive potential than on Pt single-crystals, with various minor waves preceding the main wave (located in the window 0.04–0.17 V vs. RHE). This observation agrees with the decreased reactivity toward nitrous acid reduction for a PtRh 90:10 alloy with respect to bare Pt, as reported by da Cunha et al. [22]. NO adlayers were formed upon contact with the acidic $HNO_2$ solution and these were stripped from the electrode during a negative-going sweep. The peaks recorded in this experiment paralleled those of the continuous reduction, suggesting that bulk $HNO_2$ reduction can only take place if the adsorbate is stripped. Additionally, a peculiar behavior of two basal planes was reported [21]: clean Rh (1 0 0) could not be completely recovered after adsorbate stripping, pointing to the presence of a very resilient adsorbate species or to the poisoning by partially reduced adsorbates; on the other hand Rh (1 1 0) did not exhibit any vibrational signal typical of $NO_{ad}$ in the FTIR spectra. Rodes et al. speculated that the latter phenomenon could be explained by the coexistence of molecular and dissociated (into $N_{ad}$ and $O_{ad}$) NO. UHV surface-science studies reviewed by Brown and King [23] support the validity of this hypothesis for low-coverage $NO_{ad}$, and de Vooys et al. [24] have speculated on the occurrence of NO decomposition on Rh electrodes. Literature on product distribution during nitrite/nitrous acid reduction on Rh is scarce: da Cunha et al. [22] showed that, for the PtRh 90:10 alloy, NO and $N_2O$ are evolved simultaneously before N–H coupling takes place at potentials immediately preceding hydrogen evolution, with the formation of $NH_3OH^+$ or $NH_4^+$. A Rh/Pt cathode combined to a Nafion membrane and a Pt anode also displays a high selectivity to $NH_4^+$, which increases with increasing pH. A predominant formation of $NH_3$ on graphite-supported Rh has been reported by Brylev et al. [16] for neutral media.

In this paper, we report new findings concerning the nitrite/nitrous acid reduction on Rh as a function of pH, both with respect to the reaction mechanism and the product distribution, as determined by means of rotating ring-disk electrodes (RRDE) and on-line electrochemical mass spectrometry (OLEMS). Similar to Pt electrodes, in acidic media the reactivity is dominated by NO, generated by decomposition of $HNO_2$; on the other hand, $NO_2^-$ directly takes part in the reduction pathway in alkaline media. In both cases, reduction of the N(III) species leads to ammonia.

## 2. Experimental

All glassware was cleaned following a standard procedure [25] to remove all traces of organic contaminations. Electrolyte solutions were prepared with Suprapur (Merck) or comparably pure (Sigma–Aldrich) electrolytes and Millipore MilliQ water (resistivity > 18.2 MΩ cm); prior to the experiments, oxygen was removed by bubbling argon (purity grade 6.0) through the solution for at least 15 min (acidic solution) or longer for alkaline solutions. Argon blanketing was used to protect the solutions during the experiments. $NaNO_2$ (99.999%, Sigma–Aldrich) was used as received and stored in a desiccator under vacuum; contact with air was kept as short as possible. In the pH range where nitrous acid decomposition takes place, concentrations reported in this paper are meant as nominal (initial); no real-time monitoring of the concentration was carried out. Phosphate buffer solutions (ionic strength 0.1 M) were prepared for the experiments in the range 2 < pH < 3; the pH was checked before and after the experiments with a Radiom-

eter Copenhagen pH meter. No noticeable pH change was observed during the experiments.

An Autolab PGSTAT20 (bi-)potentiostat was used throughout this work. Transfer and stationary experiments were carried out with Rh electrodes of various shapes (flag or bead), all at least 99.9% purity (various suppliers). The Rh flag electrode was flame-annealed and quenched in water saturated with an Ar atmosphere [10]. For all electrochemical experiments involving stationary electrodes, the counter was a platinum flag. A Reversible Hydrogen Electrode (RHE) was employed as reference electrode for all experiments, and all potentials reported in this paper are relative to the RHE.

Rotating disk gold electrodes (diameter 5 mm) were used in a Pine Instrument Ring-Disk Teflon tip equipped with a Pt ring; rotating disk (RDE) and rotating ring-disk (RRDE) experiments were performed with a Pine Instrument motor generator (MSR rotator). The experimental collection efficiency was 0.26 ± 0.03 as calculated with the reversible couple $[Fe(CN)_6]^{-4}/[Fe(CN)_6]^{-3}$. A different cleaning procedure was used for the RRDE tip, as described in a previous publication [14]. RRDE experiments involving Rh were carried out by depositing the noble metal on gold from a solution of its chloride salt. The procedure for constant-potential Rh deposition on Au is based upon the work of Shimazu et al. [26], with the following modification: the deposition was stopped when a pre-determined amount of charge was measured. This ensured that the Rh deposit still showed a mirror-like appearance. The 1 mM $RhCl_3$ solution was blanketed with Ar during the deposition. This solution was recycled as the deposition efficiency (i.e. time needed to achieve the deposition charge) improved with aging. This is a known feature of deposition baths containing noble metal chlorides and has been reported in studies dealing with electroless deposition [27]. The thin foreign metal layer on Au was removed at the end of each experiment by thorough polishing with alumina suspension (in sequence: 5–1–0.3 μm). Control experiments were performed with a polycrystalline Rh disk (diameter 6 mm) driven by a Motomatic motor: no difference was noticed with respect to the rhodium-on-gold disk used in combination with the Pine motor.

Adsorbate studies were performed using the following transfer procedure [28]: the flag electrode was immersed in a nitrite-containing solution (0.8 mM) of a chosen electrolyte under potential control for 120 s, rinsed and then protected with a droplet of water during the transfer to another cell containing clean electrolyte. Adsorbates thus formed are known to undergo the transfer unscathed [24]. The nitrite concentration chosen for the adsorption step equals the one used in stationary continuous reduction experiments (0.8 mM).

On-line electrochemical mass spectrometry (OLEMS) [29] measurements were performed on an EvoLution mass spectrometer system (European Spectrometry Systems Ltd.). The system consists of a Prisma QMS200 (Pfeiffer), brought to vacuum with a TMH-071P turbo molecular pump (60 l/s, Pfeiffer) and a Duo 2.5 rotary vane pump (2.5 m$^3$/h, Pfeiffer). During measurements, the pressure inside the MS was $1–5 \times 10^{-6}$ mbar. Pretreatment procedures and details were published in a previous paper [14]. For OLEMS experiments, an Rh bead type electrode was used.

## 3. Results

### 3.1. Acidic media

In the (mildly) acidic pH range, it is more appropriate to refer to nitrous acid, as this is the predominant species [9].

#### 3.1.1. Nitrous acid reduction and adsorbate stripping at stationary Rh electrodes

Nitrous acid/nitrite reduction was first investigated at stationary Rh electrodes in (mildly) acidic media (0.5 M $H_2SO_4$ and

0.1 M phosphate buffer, pH 3). $HClO_4$ was not used in this work because it is known that Rh catalyzes the decomposition of $ClO_4^-$ anions to $Cl^-$ [30]. A transfer experiment was performed to assess the formation of adsorbed species during nitrite reduction in 0.5 M $H_2SO_4$, and the voltammetric profile of the adsorbate stripping is shown in Fig. 1. A broad reduction peak can be seen, followed by two other minor signals. It must be noted that a single sweep down to 0.05 V is not sufficient to recover the blank voltammogram completely; in particular, the minor "shoulder" signal at higher potentials is shifted and its charge is diminished. This phenomenon is likely due to the "irreversible poisoning" of Rh (1 0 0) facets [21] mentioned in Section 1. The identification of the adsorbate as NO is supported by the dependence of the stripping peak potential on the stripping scan rate in 0.1 M $H_2SO_4$. This plot, shown in the inset of Fig. 1, is equivalent to a "Tafel plot", and yields a slope of $77 \pm 4$ mV dec$^{-1}$, reasonably close to the value published for NO in the same electrolyte [24]. The stripping charge (in 0.1 M $H_2SO_4$) corrected for hydrogen adsorption [28] corresponds to a NO coverage of 0.62 ML.

An increase in pH, which will minimize the decomposition of nitrous acid, has no major effect on the formation of adsorbed NO from a (mildly) acidic nitrite solution. The estimated NO coverage and the stripping charge are largely independent of the pH of the nitrite solution; moreover, also the position of the stripping peak potential does not change with the pH on the RHE scale, thus showing a trivial "Nernstian" dependence on the pH.

### 3.1.2. Nitrous acid reduction at RRDE

Evidence for diffusion limitations in the reduction of nitrous acid can be found in the literature [14,31]; therefore, additional experiments with rotating Rh electrodes were carried out to study the reduction of nitrous acid under controlled diffusion conditions. Moreover, the RRDE technique allows the detection of those soluble reaction products that are electroactive at the Pt ring; in acidic media, the detectable product is mainly $NH_3OH^+$ [14,31].

The voltammetric profile for the reduction of 50 μM $NaNO_2$ in 0.5 M $H_2SO_4$ is reported in Fig. 2, along with the cyclic voltammetry of a Pt disk electrode in the same solution. A lower concentration (with respect to the experiment described in Section 3.1.1) minimizes the influence of the decomposition of nitrous acid [14]; in addition, the cyclic voltammogram was recorded immediately after the addition of $NaNO_2$. The comparison of the two voltammograms shows that Rh does not display the first wave (0.3 < E < 0.5 V) typical of Pt, which has been associated with the
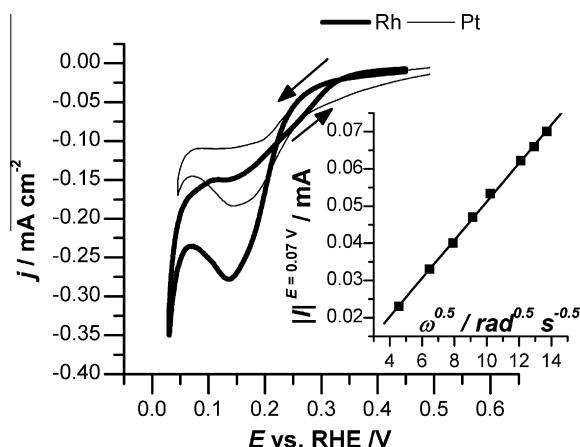


**Fig. 2.** Reduction profile of 50 μM $NaNO_2$ in 0.5 M $H_2SO_4$ at a rotating Rh electrode (bold line) compared to a rotating Pt electrode (thin line), $v = 10$ mV/s, $\omega = 900$ rpm. Inset: Levich plot at $E = 0.07$ V.

formation of $N_2O$ [14]. A broad reduction wave dominates the voltammogram for both metals, with a slightly more positive onset potential on Pt than on Rh; nevertheless, Rh reaches a larger current, both for the peak-shaped signal in the negative-going sweep and for the plateau-like region in the positive-going sweep. Lastly, the current of the return sweep is larger (in absolute value) than that of the forward sweep for E > 0.20 V, suggesting that the activity on Rh increases after an excursion to more negative potentials.

The dependence of the current on the rotation rate was studied at a potential in the plateau-like region; the Levich equation [32] is verified at $E = 0.07$ V, giving a straight line with zero intercept (inset of Fig. 2). This indicates a purely diffusion-controlled reaction, whose n value is equal to $5.3 \pm 0.1$; it seems reasonable to assume that the major reaction product is $NH_4^+$ (6 electrons) and that the uncertainty on the value of n could arise from the overestimation of the nitrous acid concentration, as already mentioned in a previous paper [14]. Moreover, the comparison of the plateau-like regions of the voltammograms of the two metals (recorded under the same conditions) shows a ca. 3/2 ratio between the currents of Rh and Pt, respectively. As the four-electron reaction to $NH_3OH^+$ was demonstrated at a Pt electrode [14], this observation would support a 6-electron reaction on Rh. Lastly, RDE experiments at a mildly acidic pH (2.7) in the micromolar nitrite concentration range, yielded a similar voltammetric profile; the number of electrons calculated from the Levich plot was higher i.e. $5.5 \pm 0.1$.

RRDE experiments with a Pt ring were aimed at detecting the formation of $NH_3OH^+$; this molecule is easily oxidized on a Pt electrode in acidic media [33]. The nitrite concentration was in the millimolar range (0.8 mM). The comparison of the cyclic voltammograms for the Pt ring electrode with the disk at open circuit potential and the disk kept at constant potential in the diffusion-limited potential region ($E_{disk} = 0.07$ V) is shown in Fig. 3. The two voltammetric profiles only differ in the 0–0.2 V and in the 1.1–1.5 V ranges, the voltammograms being identical in the 0.2–1.1 V range. Both at lower potentials and at higher potentials, only a shielding of the ring current is observed when $E_{disk} = 0.07$ V, with no change in features; the loop expected in the anodic current at E > 1 V when hydroxylamine is formed in a nitrite-containing solution [14,31] is absent. This result supports the identification of the reaction product of the reduction of $HNO_2$ on Rh at low potentials as $NH_4^+$. In addition (see inset in Fig. 3), another experiment was carried out to detect the potential range of $HNO_2$ consumption, as previously reported for Pt [14]. The ring current at constant potential was measured ($E = 0.08$ V) as an indication of $HNO_2$ consumption [14], while the disk potential was scanned. Two regions,
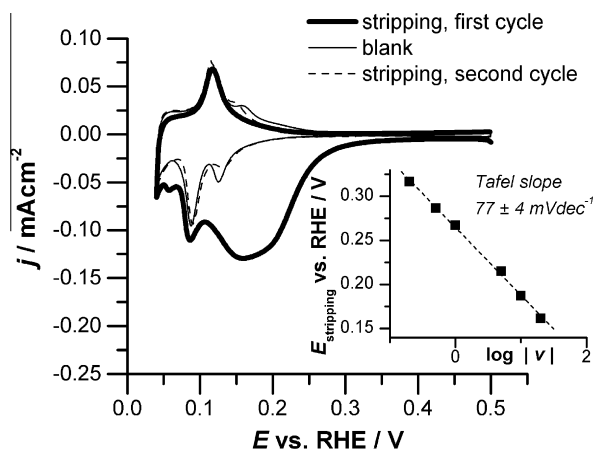


**Fig. 1.** Voltammetric profile for the first two cycles of adsorbate stripping (bold line, first cycle ; dashed line, second cycle) on a polycrystalline Rh electrode in 0.1 M $H_2SO_4$, $v = 20$ mV/s (blank CV: thin line). Inset: Tafel slope for adsorbate stripping in the same electrolyte.

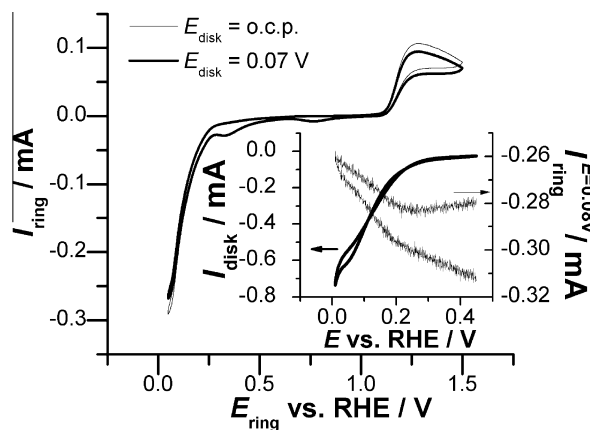**Fig. 3.** Profile of the ring current during a shielding experiment ($\omega = 900$ rpm, $v = 10$ mV/s) in 0.5 M $H_2SO_4$ + 0.8 mM $NaNO_2$. Bold line depicts $I_{ring}$ with $E_{disk} = 0.07$ V, and thin line with disk at open circuit potential (o.c.p.). Inset: comparison between the current recorded at a Rh disk ($I_{disk}$, bold line) during potential scan ($\omega = 1200$ rpm, $v = 10$ mV/s) and a Pt ring ($I_{ring}$, $E_{ring} = 0.08$ V, thin line) in the same solution as the main figure.

characterized by different slopes of the ring current, can be observed: in the range $0.2 < E < 0.45$ V the ring current decreases more slowly than in the 0.0–0.2 V region, where the direct consumption of $HNO_2$ is more massive. A clear difference is also visible between the negative-going and the positive-going sweep, with a steeper slope in the former; this discrepancy between the two sweeps, also observed for Pt [14], would suggest that a larger amount of $HNO_2$ is involved in the reaction during the negative-going half of the cycle.

### 3.1.3. On-line electrochemical mass spectrometry (OLEMS)

OLEMS experiments were carried out in order to follow the formation of gaseous products, such as $N_2$ ($m/z = 28$), NO ($m/z = 30$) and $N_2O$ ($m/z = 44$), as previously described for platinum electrodes [14]. The results displayed in Fig. 4 refer to the reduction of nitrite (0.8 mM) in 0.5 M $H_2SO_4$. Starting from 0.6 V, the increase in $m/z$ 44 can clearly be seen, with a region of maximum intensity ranging from 0.35 to 0.45 V both in the forward and in the negative direction. The signal for $N_2O$ rapidly decreases for $E < 0.32$ and reaches zero for potentials lower than 0.2 V, that is, in correspondence to the onset of the broad reduction wave. In addition, the potential range of $N_2O$ formation coincides with that of slow decrease of ring current (see Fig. 3), as discussed in the previous section, and the formation of $N_2O$ in the negative-going scan exceeds that of the positive-going scan. The analysis of $m/z$ 30, on the other hand, shows unambiguously that NO is present in the solution and is consumed during the formation of $N_2O$: in fact, the NO current signal decreases monotonically during the negative-going potential sweep, until a constant, non-zero value is reached for potentials lower than 0.20 V. It must be noted that NO is also a fragmentation product of $N_2O$; here, the correction for this interference was not carried out, and the additional contribution to $m/z$ 30 due to $N_2O$ fragmentation is clearly visible in the range 0.35–0.45 V, causing a change in the slope of the current signal. The detection of $NH_4^+$ would be particularly interesting to support the detection of this product by RRDE as described earlier, but it is extremely difficult in this pH range, this ion being largely undissociated and therefore non-volatile. As a consequence, the OLEMS experiment was repeated at pH 3: under these conditions, detection of a fragment of $NH_3$ ($m/z$ 15, which is not affected by interferences from $H_2O$ [34]), was possible. This fragment is reported to be equivalent to 10% of the main $m/z$ 17 species [35]. The formation of $NH_3$ takes place for $E < 0.20$ V. The current profiles are identical to those of
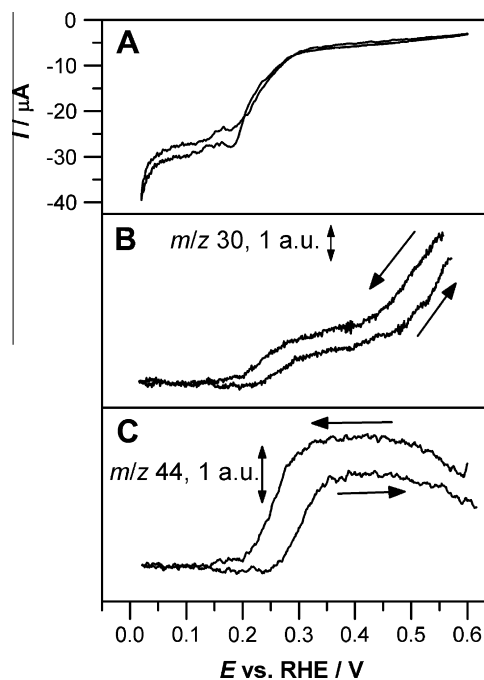


**Fig. 4.** Cyclic voltammetry during OLEMS measurements (A) and ion current profiles for $m/z = 30$ (B) and $m/z = 44$ (C) in 0.5 M $H_2SO_4$ containing 0.8 mM $NaNO_2$. The working electrode was a polycrystalline Rh bead electrode, $v = 1$ mV/s. The arrows indicate the direction of the potential sweep.

Fig. 8 (vide infra, OLEMS at pH 13), although the intensity of the $m/z$ 15 signal is far weaker at pH 3 than at pH 13. Moreover, in the pH 3 buffer we also observed a less massive formation of gaseous molecules; this is directly caused by the decreased magnitude of nitrous acid decomposition, both due to a decreased prevalence of $HNO_2$ ($NO_2^-$ roughly accounts for 1/3 of the N(III) species at this pH) and to a more sluggish decomposition of $HNO_2$ itself. Because of intrinsic limitations of the current OLEMS setup, described in previous publications [29,36], a quantitative comparison of the gaseous products measured in two different experiments cannot be obtained. However, Table 1 compares the results of a semi-quantitative internal calibration based on the currents of hydrogen evolution ($m/z$ 2) measured in 0.5 M $H_2SO_4$ and the pH 3 buffer at the same potential ($E = 0.06$ V). The Table clearly shows that although the (baseline-corrected) current for hydrogen evolution is in the same order of magnitude for both pH values, the normalized $N_2O$ current is 10 times higher for the more acidic electrolyte.

### 3.2. Alkaline media

#### 3.2.1. Nitrite reduction at RRDE

The reduction of nitrite (50 µM) at a rotating Rh disk electrode in 0.1 M NaOH is shown in Fig. 5 (inset). The shape of the current signal approaches a sigmoidal curve, with a broad peak feature at 0.15 V in the negative-going (forward) scan and a plateau-like region around 0.1 V in the positive-going (backward) scan. The onset potential is approximately at 0.4 V, and at the contact potential (0.5 or 0.45 V) a small reduction current is already recorded. This profile can be compared to that recorded on polycrystalline Pt electrodes in the same electrolyte, published elsewhere [14], which instead featured the presence of a narrow peak (both in the positive- and in the negative-going scan) centered at 0.2 V, as can be also seen in the Pt ring profile reported in Fig. 5 (see below). The peculiar feature of Rh, therefore, is the presence of a remarkable reduction activity at potentials where Pt is inhibited, probably by the competition between nitrite reduction and hydrogen adsorption [37].

**Table 1**
Comparison of the normalized NO and N$_2$O ion currents for a 0.5 M H$_2$SO$_4$ and a 0.1 M phosphate buffer solution. The first column reports the baseline-corrected ion current during H$_2$ evolution, measured in the two electrolytes. These values were used to normalize the NO and N$_2$O currents.

| Electrolyte | Baseline-corrected ion current for $m/z$ 2, value at $E = 0.06$ V (vs. RHE)/A | Normalized current for $m/z$ 30 (NO) | Normalized current for $m/z$ 44 (N$_2$O) |
|---|---|---|---|
| 0.1 M phosphate buffer, pH 3 | $3.20 \times 10^{-12}$ | 0.17 | 0.28 |
| 0.5 M H$_2$SO$_4$ | $2.00 \times 10^{-12}$ | 4.03 | 2.25 |
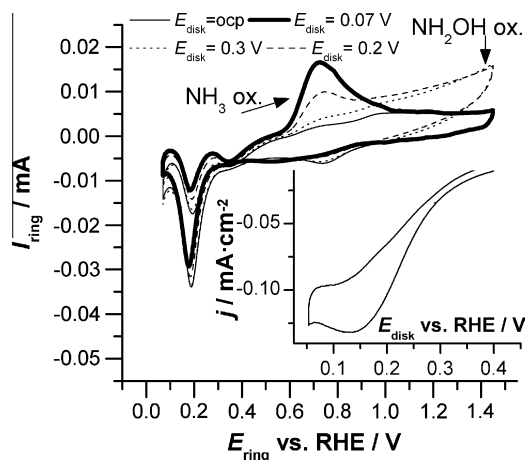


**Fig. 5.** Profile of the ring current during a shielding experiment ($\omega = 900$ rpm, $v = 10$ mV/s) in 0.1 M NaOH + 0.8 mM NaNO$_2$. $I_{ring}$ is shown for various $E_{disk}$ values. Inset: current recorded at a Rh disk during potential scan ($\omega = 900$ rpm, $v = 10$ mV/s) in 0.1 M NaOH, 50 μM NaNO$_2$.

The influence of parameters such as reactant concentration and rotation rate on the current was investigated, although a preliminary comment must be made. When recording the current at a constant potential in the pseudo-plateau region (see Fig. 5, inset), $I$ decreased slowly but continuously with time. The current decrease over a fixed amount of time was found to be dependent on the rotation rate, with a larger increase for faster rotation rates. Constant-potential measurements were therefore carried out as fast as possible. The pseudo-limiting current measured at $E = 0.07$ V and $\omega = 900$ rpm increases with an increase in concentration, giving an apparent reaction order of 0.65 in the NO$_2^-$ concentration range 25–125 μM, a reaction order lower than 1 being often indicative of the presence of a step involving an adsorbed (poisoning) species. The current measured at a constant potential ($E = 0.07$ V) in the micromolar concentration range (75 μM) is a function of $\omega$ in the range 200–2000 rpm, whereas for higher $\omega$, $I$ progressively becomes independent of $\omega$. Rotation rates were changed randomly to avoid the interfering influence of the aforementioned poisoning. The influence of rotation rate was also studied with linear sweep voltammetry, which showed that $I$ is a function of $\omega$ for potentials lower than $E = 0.20$ V.

Rotating ring-disk experiments are particularly important for the detection of soluble reduction products electroactive on the Pt ring: NH$_2$OH and NH$_3$. These species are characterized by an oxidation current around $E = 0.65$ V for NH$_3$ in alkaline media [9,38,39] and, for hydroxylamine, above ca. $E = 1$ V both in acidic media and alkaline media [9]. The oxidation of NO$_2^-$ on the Pt ring is highly inhibited in alkaline media, presumably due to the formation of the oxide layer [9,40], and so, contrary to acidic media, it does not interfere with other oxidative processes. The evolution of the cyclic voltammetry profile at the ring electrode as a function of the applied potential at the Rh disk is shown in Fig. 5. A change
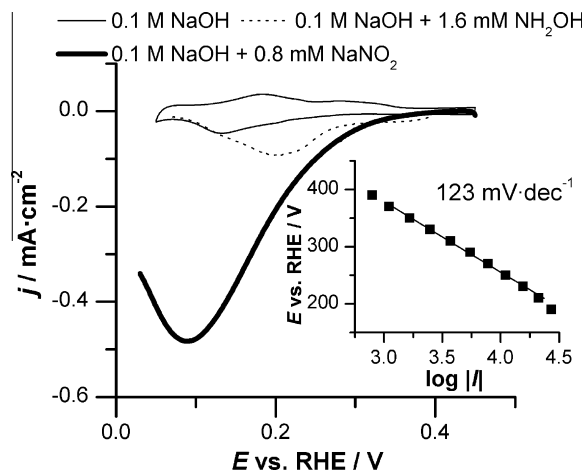


**Fig. 6.** Comparison of the voltammetric profiles of a stationary Rh electrode in 0.1 M NaOH (blank, thin line), with the addition of 0.8 mM NaNO$_2$ (bold line) or 1.6 mM NH$_2$OH (dotted line). $v = 20$ mV/s. Inset: Tafel slope analysis for a Rh electrode immersed in a 0.1 M NaOH + 0.8 mM NaNO$_2$ solution. Potential program: steps of 10 mV/min.

of the ring current signal, with respect to the situation at $E_{disk}$ = o.c.p., can already be appreciated at disk potentials as low as 0.3 V, which corresponds to the Tafel slope region discussed in the previous section. An increased oxidation current in the potential region $1 < E_{ring} < 1.5$ V is evident, along with a shielding of the peak-shaped reduction signal at $E_{ring} = 0.19$ V. This pattern was already reported for nitrite reduction on Pt and was then ascribed to the formation of NH$_2$OH [14]. A decrease in the disk potential to 0.2 V causes the appearance of an oxidation peak centered at 0.69 V, while no change takes place in the higher range of ring potentials. A full selectivity to NH$_3$ is achieved on the verge of hydrogen evolution (0.07 V), as at that disk potential the ammonia oxidation peak is the only oxidation feature in the ring voltammetry. The shielding of the nitrite reduction current at the ring increases with decreasing potential, indicating that the consumption of nitrite at the disk increases. We can hence conclude from these RRDE data, that the reduction of NO$_2^-$ proceeds to give NH$_2$OH at low overpotential, but to NH$_3$ at more negative potentials, with an intermediate potential region with the formation of both products.

### 3.2.2. Nitrite reduction at stationary rhodium electrodes

Further experiments were carried out at stationary Rh electrodes. The current profile recorded at a stationary Rh electrode immersed in a 0.1 M NaOH solution containing 0.8 mM NaNO$_2$ is shown in Fig. 6. A single peak centered at 0.09 V can be observed; its peak current was found to be dependent on the square root of the scan rate. A Tafel slope analysis was carried out by measuring the current during steady-state reduction of 0.8 mM NaNO$_2$ in 0.1 M NaOH; the starting potential was $E = 0.4$ V and $E$ was stepped down by 10 mV per minute. Care was taken to avoid the interference of products at the counter-electrode, which was isolated in a separate compartment equipped with a glass frit. The Tafel slope was equal to 123 mV dec$^{-1}$, with a linear region extending from $E = 0.35$ V to $E = 0.20$ V (inset of Fig. 6). The influence of diffusive processes at the stationary electrode may be ruled out as the logarithmic plots of the various voltammograms recorded at a RDE reproducibly yield a slope of 120 mV dec$^{-1}$ in the same potential region. This information suggests that the rate-determining step of the process is the first electron transfer, which in our case would correspond to the formation of NO, as in

$$H_2O + NO_{2(ads)}^- + e^- \rightarrow NO_{ads} + 2OH^- \tag{1}$$
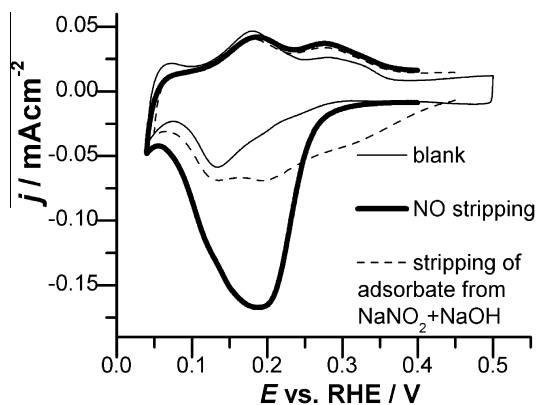
**Fig. 7.** Voltammetric profile for the stripping of adsorbed NO in 0.1 M NaOH (bold line, first cycle) on a Rh electrode, compared to the stripping (in the same electrolyte) of the adsorbate generated in 0.1 M NaOH + 0.8 mM NaNO$_2$ (dotted line) and the blank voltammogram (thin line). $v$ = 20 mV/s.
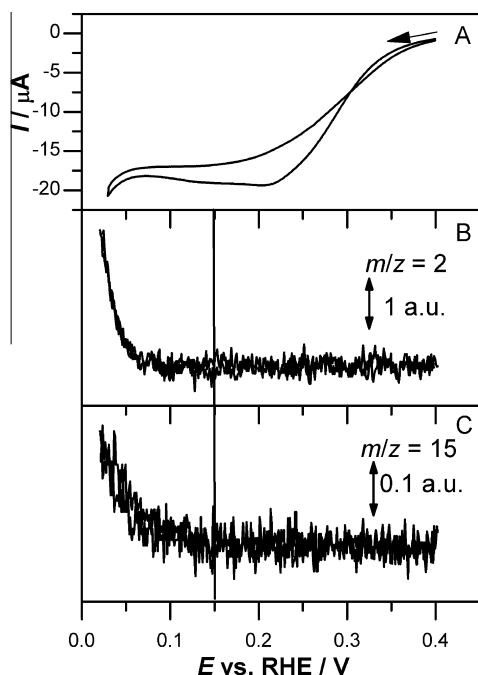


**Fig. 8.** Cyclic voltammetry during OLEMS measurements (A) and ion current profiles for $m/z$ = 2 (B) and $m/z$ = 15 (C) in 0.1 M NaOH containing 0.8 mM NaNO$_2$. The working electrode was a polycrystalline Rh bead electrode, $v$ = 1 mV/s. The arrow indicates the beginning of the potential sweep.

The NO formed is likely to occur as adsorbate, and for this reason a characterization study of the stripping of an NO layer in alkaline media was carried out. The NO adlayer was generated by contacting the electrode with a nitrite-containing 0.5 M H$_2$SO$_4$ solution. The stripping voltammogram of this NO adsorbate in 0.1 M NaOH features a single peak (Fig. 7). The dependence of the peak potential ($E_{peak}$), $\delta E_{peak}/\delta \log v$, was equal to 90 mV dec$^{-1}$, somewhat higher than the corresponding slope in acidic media (comparable to what reported by de Vooys et al. [24]).

Similar experiments were carried out in order to ascertain the state of the NO adsorbate on Rh at the beginning of the reduction of nitrite in alkaline media by keeping the electrode at $E$ = 0.45 V in the alkaline nitrite solution for 120 s and then transferring it to clean alkaline electrolyte. The stripping voltammogram was then recorded and compared to the stripping of a full NO adlayer (as generated in acidic solution) in the 0.1 M NaOH solution. The strip-

ping charge for a saturated NO adlayer (formed in acidic nitrite solutions) is much larger than the charge measured during stripping of the adsorbed species generated in an alkaline NaNO$_2$ solution. Nevertheless, in both cases, the peak of NO reduction is clearly visible, centered at $E$ = 0.2 V. The voltammetric profile for the adsorbates formed in the alkaline NaNO$_2$ solution also displays a reduction current in the region preceding the main stripping peak (i.e. at $E$ > 0.3 V), perhaps due to the reduction of adsorbed NO$_2^-$ ions.

Considering that NH$_2$OH is a product of NO$_2^-$ reduction in the range 0.2 < $E$ < 0.3 V, we also investigated, by means of a simple cyclic voltammetry experiment, the reduction of a 1.6 mM NH$_2$OH solution, prepared by dissolving (NH$_3$OH)$_2$SO$_4$ in the alkaline working solution, at a Rh electrode. The reduction profile displays a broad peak with an onset potential of $E$ = 0.25 V (dotted line in Fig. 6), which is more positive than the potential at which NH$_3$ starts to be produced, according to RRDE data ($E$ = 0.2 V).

### 3.2.3. On-line electrochemical mass spectrometry (OLEMS)

OLEMS experiments were carried out in order to obtain additional evidence for the formation of NH$_3$ during nitrite reduction in 0.1 M NaOH. Fig. 8 shows the MS ion current for the ammonia fragment having $m/z$ = 15, along with the signal for hydrogen formation. The comparison to the latter is important to test the occurrence of the formation of ammonia due to catalytic hydrogenation of nitrite on rhodium by hydrogen, which was earlier mentioned by Brylev et al. [16]. The data in Fig. 8 clearly demonstrate that nitrite is reduced to ammonia on rhodium for $E$ < 0.16 V, whereas hydrogen evolution only commences for $E$ < 0.07 V. Obviously, hydrogen generated *in situ* will eventually reduce nitrite ions to ammonia, and the catalytic hydrogenation will probably be active as an alternative pathway at such low potentials. It must be noted that the detection of NH$_3$ shows a certain delay with respect to the voltammetric current profile, which reaches its maximum value already at $E$ = 0.22 V during the negative-going scan. This may be due to the difficulty of detecting a minor fragment of a highly water soluble (and thus repelled by the membrane of the OLEMS tip) molecule such as NH$_3$. The current branch stretching from 0.4 V to 0.22 V must be related to the formation of surface species or short-lived intermediates (see previous sections), such as NH$_2$OH: during the OLEMS experiment, zero ion current was recorded for (the fragments of) NO, N$_2$O, N$_2$ and NH$_2$OH.

## 4. Discussion

### 4.1. Acidic media

The reduction of nitrous acid/nitrite at rhodium electrodes in acidic media can be discussed by dividing the potential region into two sections characterized by different main products: a high-potential region (0.35–0.55 V), where N$_2$O formation is detected, and the potential range immediately preceding hydrogen evolution ($E$ < 0.15 V), where NH$_4^+$ formation predominates.

### 4.1.1. N$_2$O evolution and NO adlayer

In a previous paper dealing with nitrite reduction at Pt electrodes [14], we reported the presence of a high-potential first-wave signal in acidic media, corresponding to the formation of N$_2$O as measured during an OLEMS experiment. In the present study, the formation of N$_2$O (in the same potential region as platinum) is observed, although not accompanied by a similar pre-wave. This fact may arise from a combination of causes. In the first place, the presence of anions or a partially oxidized surface (although we tend to exclude the latter case for our experiments) could mask the current of N$_2$O formation. The presence of anions

in the potential range of $N_2O$ formation is certain: rhodium has a lower PZC than platinum (reported in the literature as low as 0.17 V in a pH 2.5 solution [41]), thus inducing a stronger anion adsorption. Secondly, de Vooys et al. [24] showed that $N_2O$ formation on rhodium differs mechanistically from the same reaction on platinum, as evidenced by the difference in the Tafel slope for NO reduction to $N_2O$ on the two metals. The value reported for rhodium, much higher than 120 mV dec$^{-1}$, was tentatively assigned to the presence of a rate-determining chemical step (the formation of $(NO)_2$) preceding the first electron transfer. This suggestion can be correlated with the larger NO coverage observed on Rh than on Pt and with the metal–nitrogen interaction, which is stronger for Rh than for Pt, as mentioned by Petrii and Safonova [37] in relation to nitrate reduction, and confirmed by density functional theory calculations of Zeng et al. [42] showing that the adsorption energy of NO on Rh (1 1 1) is the highest among the transition metals. We may thus hypothesize that the formation of a NO dimer, according to the scheme

$$NO_{ads} + NO_{aq} = (NO)_{2,ads} \qquad (2)$$

involves the weakening of the existing metal–nitrogen bond upon reaction with the second NO molecule coming from the solution phase. A strong Rh–N bond would disfavor this reaction, thus rendering the NO dimer formation slow enough to become the rate-determining step of the entire $N_2O$ evolution process. The effect of the pH on the formation of gaseous molecules is evident from the trend of the normalized ion currents shown in Table 1: the decomposition of nitrous acid is slower at higher pH.

When exposed to a solution containing NO, rhodium readily forms robust adlayers, with NO possibly being partially dissociated [23] into atomic species which are more resilient to reductive stripping than molecular NO. The presence of such species, for example, would explain the fact that, contrary to platinum, a single excursion into the region of NO reduction is not sufficient to recover the profile for clean Rh. In addition, the higher affinity of rhodium toward the chemisorption of NO is shown by the dependence of the NO coverage on the pH of the nitrite-containing generating solution: for Pt, a significant decrease in $\theta_{NO}$ is observed when the adlayer is generated in a nitrite-containing pH 3 buffer [14], whereas for Rh in alkaline media the NO coverage is still substantial compared to acidic media (see Section 3).

The tendency to form $N_2O$ during nitrous acid reduction at a Rh electrode is in agreement with previous observations by Brylev et al. [16], who first recognized the remarkable decrease in the current efficiency to nitrite in mildly acidic solutions, due to a parallel pathway involving $HNO_2$ decomposition, NO generation and electrochemical $N_2O$ formation. A recent paper by Hasnat et al. [20] also shows that the selectivity to ammonia during nitrite reduction at Pt/Rh cathode decreases with decreasing pH, along with increased formation of gaseous side products.

### 4.1.2. $NH_4^+$ formation

The formation of $NH_4^+$ is peculiar to nitrous acid reduction in acidic media at a Rh electrode; Pt, on the other hand, reduces $HNO_2$ to $NH_3OH^+$ [14]. A comparative analysis of the behavior of the two metals is informative and allows a broader discussion on the similarities of $HNO_2$ reduction with other processes involving nitrogen-containing molecules. At the starting potential of Fig. 3 (RDE), both Rh and Pt are covered with an NO adlayer: during the negative-going sweep, the reactivity of this adsorbed molecule dominates, and the current will reflect the reductive removal of NO, and the reduction of $HNO_2$ – if it ever takes place – is overlapping this process. Once the NO layer has been removed, the "clean" metal is able to perform the direct reduction of $HNO_2$, which is a diffusion-limited process for both Rh and Pt. This observation can
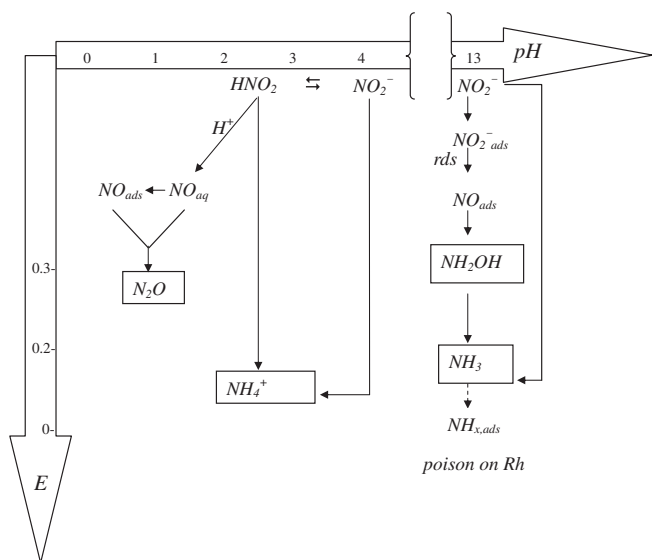
be paralleled with the reduction of $NO_3^-$ at noble metal electrodes in acidic media: for the latter process, the removal of the first oxygen atom ($NO_3^-$ to $NO_2^-$) is the rate-determining step [10]. Therefore, it is not surprising that, as we observed in the present study in acidic media and at micromolar $NO_2^-$ concentrations, the direct reaction of $HNO_2$ is a fast, diffusion-controlled process. The different product selectivities of the two metals reflect a difference in the ability of Pt and Rh to adsorb NO in a dissociative fashion: Rh displays a higher tendency to form atomic N and O species upon exposure to NO than Pt [23,43]. Since the breaking of an N–O bond discriminates the formation of $NH_2OH$ from $NH_3$, our findings are further evidence of the different intrinsic properties of Rh and Pt.

### 4.2. Alkaline media

The low selectivity towards nitrogen oxides and the high selectivity towards $NH_3$ during $NO_2^-$ (or $NO_3^-$) reduction at a Rh electrode in alkaline media is in agreement with previous reports of various rhodium-containing systems [16,20,22]. Our results indicate that the electrode, when immersed in a nitrite-containing alkaline solution at the starting potential (0.45 V or 0.5 V), is covered by adsorbed $NO_2^-$ and NO, the latter generated by reduction of the former. No NO was detected in the MS setup during the reduction of $NO_2^-$, and therefore this intermediate is never desorbed, being reduced to more hydrogenated compounds directly on the Rh surface. Since NO does not desorb, the formation of $N_2O$ is not observed [24]. The presence of adsorbed $NO_2^-$ on Rh around 0.4 V is not surprising, given the PZC of polycrystalline Rh in alkaline media (0.23 V at pH 12.7 [41]). Hydroxide ions will be the only competing species for the adsorption of $NO_2^-$ ions. The strong NO adsorption can be ascribed to the favorable interaction between the Rh surface and NO, as explained in the previous sections. The presence of adsorbed species would also explain the presence of excess reduction charge during adsorbate stripping (Fig. 7). The value of the Tafel slope recorded at the beginning of the $NO_2^-$ reduction process supports the hypothesis that the first electron transfer (to form NO) is rate-determining during the reduction process, at least in the potential range corresponding to $NH_2OH$ formation.

The product analysis performed with RRDE and OLEMS is crucial for the understanding of the overall reaction mechanism. As discussed in the previous sections, Rh is able to break the N–O bond and hydrogenate $NO_2^-$ completely to $NH_3$. RRDE and OLEMS show that ammonia formation starts to take place only for $E \leqslant 0.20$ V, similar to the behavior in acidic media, where the formation of nitrogen oxides dominates for higher potentials. However, in the case of alkaline media RRDE experiments prove that a molecule oxidizable at a Pt ring is generated at $E = 0.3$ V from the reduction of $NO_2^-$ at the Rh disk. This observation agrees with the electrochemical behavior of $NH_2OH$, for which the onset potential of reduction on Rh in alkaline media is approximately 0.25 V. In the $NH_2OH$ forming region, in addition, the shielding of the $NO_2^-$ reduction current at the ring (Fig. 5) is much lower than for lower potentials, evidencing a lower rate of consumption of nitrite at the disk.

The details of the process leading to $NH_3$ in the low-potential region are somewhat elusive, given the overlapping effect of the electrode poisoning. However, the data may suggest that a kinetically mixed process is active, with a contribution of the diffusion of $NO_2^-$ ions to the electrode as highlighted by the $I_p$ vs. $v^{0.5}$ dependency and by the influence of the rotation rate on the current measured in the ammonia-formation reaction. In addition, the observed reaction order, minor than 1, may be ascribed to the involvement of an adsorbed intermediate, whose nature cannot be further detailed without the aid of spectroscopic techniques. The low-potential formation of $NH_3$, and its similarity to the

**Scheme 1.** Mechanistic pathways for $NO_2^-$/$HNO_2$ reduction at a polycrystalline Rh electrode as a function of pH and $E$.

pH- and potential-dependent reaction mechanism as shown in Scheme 1. In acidic media, there is a competition between $HNO_2$/$NO_2^-$ direct reduction and $N_2O$ formation via NO generated in the aqueous phase by the acid-catalyzed decomposition of $HNO_2$. $NH_3$ is the major product at potentials close to hydrogen evolution, whereas $N_2O$ predominates between 0.3 and 0.5 V. In alkaline media, $NO_2^-$ is the only reducible species present in the solution: its reduction yields $NH_3$ for $E < 0.20$ V, which may poison the Rh electrode by forming $NH_{x,ads}$ species. The formation of the intermediates $NO_{ads}$ and $NH_2OH$ was also observed. The mechanistic information and the pH-dependent product distribution obtained in the present study corroborate the results of previous works on electrochemical reduction of $NO_3^-$ on Rh: after the rate-determining step $NO_3^- \rightarrow NO_2^-$, the reduction of $NO_2^-$, which is heavily influenced by pH, will play the role of selectivity-determining step, with a higher selectivity to gaseous products in acidic media.

## Acknowledgments

## References

[1] M.J. Moorcroft, J. Davis, R.G. Compton, Talanta 54 (2001) 785.
[2] D.M. Manassaram, L.C. Backer, D.M. Moll, Environ. Health Perspect. 114 (2006) 320.
[3] K.M. Hiscock, J.W. Lloyd, D.N. Lerner, Water Res. 25 (1991) 1099.
[4] M.N. Almasri, Environ. Impact Assess. Rev. 27 (2007) 220.
[5] V. Mateju, S. Cizinska, J. Krejci, T. Janoch, Enzyme Microb. Technol. 14 (1992) 170.
[6] M.I.M. Soares, Water, Air, Soil Pollut. 123 (2000) 183.
[7] A. Kapoor, T. Viraraghavan, J. Environ. Eng. ASCE 123 (1997) 371.
[8] J.C. Fanning, Coord. Chem. Rev. 199 (2000) 159.
[9] V. Rosca, M. Duca, M.T. de Groot, M.T.M. Koper, Chem. Rev. 109 (2009) 2209.
[10] G.E. Dima, A.C.A. de Vooys, M.T.M. Koper, J. Electroanal. Chem. 554 (2003) 15.
[11] A.C.A. de Vooys, G.L. Beltramo, B. van Riet, J.A.R. van Veen, M.T.M. Koper, Electrochim. Acta 49 (2004) 1307.
[12] G. da Silva, E.M. Kennedy, B.Z. Dlugogorski, J. Phys. Chem. A 110 (2006) 11371.
[13] R.C. Weast (Ed.), Handbook of Chemistry and Physics, The Chemical Rubber, Co., Cleveland, 1972–1973.
[14] M. Duca, V. Kavvadia, P. Rodriguez, S.C.S. Lai, T. Hoogenboom, M.T.M. Koper, J. Electroanal. Chem., in press, doi: 10.1016/j.jelechem.2010.01.019.
[15] J.Y. Park, Y.N. Lee, J. Phys. Chem. 92 (1988) 6294.
[16] O. Brylev, M. Sarrazin, L. Roue, D. Belanger, Electrochim. Acta 52 (2007) 6237.
[17] J.W. Peel, K.J. Reddy, B.P. Sullivan, J.M. Bowen, Water Res. 37 (2003) 2512.
[18] K.J. Reddy, J.P. Lin, Water Res. 34 (2000) 995.
[19] P.M. Tucker, M.J. Waite, B.E. Hayden, J. Appl. Electrochem. 34 (2004) 781.
[20] M.A. Hasnat, M.A. Islam, S.M. Borhanuddin, M.R.U. Chowdhury, M. Machida, J. Mol. Catal. A: Chem. 317 (2010) 61.
[21] A. Rodes, R. Gomez, J.M. Perez, J.M. Feliu, A. Aldaz, Electrochim. Acta 41 (1996) 729.
[22] M.C.P.M. da Cunha, F.C. Nart, Phys. Status Solidi A 187 (2001) 25.
[23] W.A. Brown, D.A. King, J. Phys. Chem. B 104 (2000) 2578.
[24] A.C.A. de Vooys, M.T.M. Koper, R.A. van Santen, J.A.R. van Veen, J. Catal. 202 (2001) 387.
[25] S.C.S. Lai, M.T.M. Koper, Faraday Discuss. 140 (2009) 399.
[26] S. Piao, Y. Kayama, Y. Nakano, K. Nakata, Y. Yoshinaga, K. Shimazu, J. Electroanal. Chem. 629 (2009) 110.
[27] I. Bianchi, E. Guerrini, S. Trasatti, Chem. Phys. 319 (2005) 192.
[28] A.C.A. de Vooys, M.T.M. Koper, R.A. van Santen, J.A.R. van Veen, Electrochim. Acta 46 (2001) 923.
[29] A.H. Wonders, T.H.M. Housmans, V. Rosca, M.T.M. Koper, J. Appl. Electrochem. 36 (2006) 1215.
[30] A. Ahmadi, R.W. Evans, G. Attard, J. Electroanal. Chem. 350 (1993) 279.
[31] R.R. Gadde, S. Bruckenstein, J. Electroanal. Chem. 50 (1974) 163.
[32] A.J. Bard, L.R. Faulkner, Electrochemical Methods: Fundamentals and Applications, second ed., John Wiley & Sons, New York, 2001.
[33] B. Piela, P.K. Wrona, J. Electrochem. Soc. 151 (2004) E69.
[34] S. Wasmus, E.J. Vasini, M. Krausa, H.T. Mishima, W. Vielstich, Electrochim. Acta 39 (1994) 23.

comparable process in acidic media, may be discussed in terms of general properties of rhodium, in particular its propensity to break the N–O bond [42,43]. $NH_3$ formation is not inhibited by hydrogen evolution, and the two processes overlap as shown by the OLEMS data; this is in stark contrast with Pt, where the observed inhibition in the reduction of various nitrogen-containing molecules at Pt in acidic [10,44] and alkaline media [14,37]. A simple explanation of this fact would ascribe it to the stronger affinity of a Rh surface towards N than H [43].

The Rh poisoning process could be a side effect of $NH_3$ formation at the potentials immediately preceding hydrogen evolution, as at these potentials $NH_3$ dehydrogenation can occur, as shown by de Vooys et al. in a study of $NH_3$ oxidation on Rh [39]. A survey of the surface-science literature on the interaction of $NH_3$ with Rh surfaces shows that this metal, in particular as Rh(1 0 0), displays an outstanding tendency to adsorb and dehydrogenate $NH_3$, forming $NH_x$ species that reside on the surface, and, according to a theoretical study by Novell-Leruth et al. [45], progressive dehydrogenation goes as far as $N_{ads}$, with the removal of the last hydrogen atom as the slowest step. N atoms have a high adsorption energy on Rh [43]. In addition, the process is relatively facile: when exposed to $NH_3$, silica-supported Rh nanoparticles form $NH_x$ adsorbates already at $T = 75$ °C [46]. $NH_4^+$ ions, on the other hand, are probably less prone to adsorption on Rh surfaces (although there is no study in the literature concerning this topic), and this would account for the absence of a similar poisoning effect in acidic media.

We can summarize the mechanism of $NO_2^-$ reduction in alkaline media as:

- $NH_2OH$ formation region: formation of NO adsorbate is rate-determining, negligible influence of rotation.
- Low-potential region: direct reduction of $NO_2^-$ to $NH_3$, kinetically mixed control, influence of diffusion. Poisoning by N or NH due to $NH_3$ dehydrogenation on Rh.

## 5. Conclusions

The reduction of $HNO_2$/$NO_2^-$ at polycrystalline Rh electrodes is influenced by the electrode potential and the pH of the solution. The results of the present study can be summarized in a general

[35] P.J. Linstrom, W.G. Mallard (Eds.), NIST Chemistry WebBook, NIST Standard Reference Database Number 69, Gaithersburg, MD, 20899. <http://webbook.nist.gov> (retrieved 18.02.10).
[36] S.C.S. Lai, M.T.M. Koper, J. Phys. Chem. Lett. 1 (2010) 1122.
[37] O.A. Petrii, T.Y. Safonova, J. Electroanal. Chem. 331 (1992) 897.
[38] K. Endo, Y. Katayama, T. Miura, Electrochim. Acta 50 (2005) 2181.
[39] A.C.A. de Vooys, M.T.M. Koper, R.A. van Santen, J.A.R. van Veen, J. Electroanal. Chem. 506 (2001) 127.
[40] B. Piela, P.K. Wrona, J. Electrochem. Soc. 149 (2002) E55.
[41] E.M. Lazarova, Elektrokhimiya 18 (1982) 1654.
[42] Z.H. Zeng, J.L.F. Da Silva, W.X. Li, Phys. Chem. Chem. Phys. 12 (2010) 2459.
[43] M. Mavrikakis, J. Rempel, J. Greeley, L.B. Hansen, J.K. Norskov, J. Chem. Phys. 117 (2002) 6737.
[44] V. Rosca, G.L. Beltramo, M.T.M. Koper, J. Electroanal. Chem. 566 (2004) 53.
[45] G. Novell-Leruth, A. Valcarcel, J. Perez-Ramirez, J.M. Ricart, J. Phys. Chem. C 111 (2007) 860.
[46] C.M. Leewis, W.M.M. Kessels, M.C.M. van de Sanden, J.W. Niemantsverdriet, Appl. Surf. Sci. 253 (2006) 572.